

# Control of Metastases via Myeloid CD39 and NK Cell Effector Function

Juming Yan<sup>1</sup>, Xian-Yang Li<sup>2</sup>, Amelia Roman Aguilera<sup>2</sup>, Christos Xiao<sup>1</sup>, Celia Jacobberger-Foissac<sup>1</sup>, Bianca Nowlan<sup>2</sup>, Simon C. Robson<sup>3</sup>, Courtney Beers<sup>4</sup>, Achim K. Moesta<sup>4</sup>, Nishamol Geetha<sup>2</sup>, Michele W.L. Teng<sup>1</sup>, and Mark J. Smyth<sup>2</sup>



## ABSTRACT

Natural killer (NK) cell protection from tumor metastases is a critical feature of the host immune response to cancer, but various immunosuppression mechanisms limit NK cell effector function. The ectoenzyme, CD39, expressed on tumor-infiltrating myeloid cells, granulocytes, and lymphocytes, including NK cells, converts extracellular ATP (eATP) into AMP and, thus, potentially suppresses eATP-mediated proinflammatory responses. A CD39-targeting monoclonal antibody (mAb) that inhibits the mouse ectoenzyme CD39 suppressed experimental and spontaneous metastases in a number of different tumor models and displayed superior antimetastatic activity compared with the CD39 inhibitor POM1 and inhibitors and mAbs that block other members of the adenosinergic family (e.g., A2AR and CD73). The antimetastatic activity of anti-CD39 was NK cell and IFN $\gamma$  dependent, and anti-CD39 enhanced the percentage

and quantity of IFN $\gamma$  produced and CD107a expression in lung-infiltrating NK cells following tumor challenge and anti-CD39 therapy. Using conditional *Cd39* gene-targeted mouse strains and adoptive NK cell transfers, we showed that CD39 expressed on bone marrow-derived myeloid cells was essential for anti-CD39's antimetastatic activity, but NK cell expression of CD39 was not critical. The eATP receptor P2X7 and the NALP3 inflammasome, including downstream IL18, were critical in the mechanism of action of anti-CD39, and the frequency of P2X7 and CD39 coexpressing lung alveolar macrophages was specifically reduced 1 day after anti-CD39 therapy. The data provide a mechanism of action involving NK cells and myeloid cells, and anti-CD39 combined with anti-PD-1, NK cell-activating cytokines IL15 or IL2, or an inhibitor of A2AR to effectively suppress tumor metastases.

## Introduction

The metastatic spread of cancer cells to distant anatomic locations is a prominent cause of cancer-related death. Metastasis is governed by cancer cell-intrinsic mechanisms, but also by micro-environmental and systemic processes, such as immunosurveillance (1). Natural killer (NK) cells play a key role in the control of metastatic dissemination, but the molecules that regulate NK cell antimetastatic activity have not been fully elucidated (1). The cell-surface ectoenzymes CD73 and CD39 are expressed on different immune cell populations and cancer cells and are responsible for regulating the balance between the proinflammatory extracellular ATP (eATP) and immunosuppressive extracellular adenosine in the tumor microenvironment (TME; ref. 2). Cancer can lead to release of high amounts of eATP through a variety of mechanisms,

including cell destruction (3), and hypoxia upregulates CD39 and CD73 (2). CD39 is a membrane-bound extracellular ectoenzyme that promotes immunosuppression by degrading adenosine triphosphate (ATP) into AMP, which is then converted to adenosine by CD73 (4). Extracellular ATP acts as a proinflammatory stimulus by agonizing P2 purinergic receptors on immune cells (5), and purinergic signaling is an important component of peripheral immune regulation (6). By signaling through purinergic receptors on immune cells, eATP functions as a danger-associated molecular pattern (DAMP) to promote innate and adaptive immune responses (3, 6). However, during inflammation, eATP is rapidly dephosphorylated by ectonucleotidases (largely CD39 and CD73), resulting in the formation of high amounts of immunosuppressive extracellular adenosine within the TME (4).

The adenosinergic pathway has been shown to regulate metastasis with roles for host CD73, adenosine 2A receptor (A2AR), and CD39 using gene-targeted mice (7–10). Therapeutic targeting of experimental and spontaneous metastases with small-molecule inhibitors of A2AR and CD39 has also revealed the importance of NK cells in the mechanism of action of these agents (8–11). Nevertheless, a direct role for CD39 expressed on NK cells has not been demonstrated in tumor metastasis. We previously developed a unique anti-mouse CD39 that inhibits CD39 ectoenzyme activity and was more effective compared with other agents targeting molecules in the adenosinergic pathway (12). Here, we describe its potent antimetastatic activity and identified the mechanism of action as being mediated via host myeloid CD39 and the eATP (P2X7)-inflammasome pathway, including downstream IL18 and NK cell effector function and IFN $\gamma$ . We eliminated a role for NK cell-expressed CD39 in this activity and demonstrated the combined activity of anti-CD39 with other NK cell-activating immunotherapies.

<sup>1</sup>Cancer Immunoregulation and Immunotherapy Laboratory, QIMR Berghofer Medical Research Institute, Herston, Queensland, Australia. <sup>2</sup>Immunology in Cancer and Infection Laboratory, QIMR Berghofer Medical Research Institute, Herston, Queensland, Australia. <sup>3</sup>Departments of Medicine and Anesthesia, Beth Israel Deaconess Medical Center, Boston, Massachusetts. <sup>4</sup>Tizona Therapeutics, San Francisco, California.

**Note:** Supplementary data for this article are available at Cancer Immunology Research Online (<http://cancerimmunolres.aacrjournals.org/>).

J. Yan and X.-Y. Li contributed equally to this article.

**Corresponding Author:** Mark J. Smyth, QIMR Berghofer Medical Research Institute, 300 Herston Road, Herston, Queensland 4006, Australia. Phone: 61-7-3845-3957; Fax: 61-7-3362-0111; E-mail: Mark.Smyth@qimrberghofer.edu.au

Cancer Immunol Res 2020;8:356–67

doi: 10.1158/2326-6066.CIR-19-0749

©2020 American Association for Cancer Research.

## Materials and Methods

### Mice

C57BL/6 and BALB/c wild-type (WT) mice were purchased from Walter and Eliza Hall Institute for Medical Research (Parkville, Australia) or the same strains bred in-house. C57BL/6 *Ptprc<sup>a</sup>* (CD45.1<sup>+</sup>) mice (purchased originally from Animal Resources Centre), C57BL/6 CD39-deficient mice (*Cd39<sup>-/-</sup>*; ref. 13), C57BL/6 CD73-deficient mice (*Cd73<sup>-/-</sup>*; ref. 14), C57BL/6 NALP3-deficient mice (*Nalp3<sup>-/-</sup>*; ref. 15), C57BL/6 P2X7-deficient mice (*P2rx7<sup>-/-</sup>*; ref. 16), C57BL/6 ASC-deficient mice (*Pycard<sup>-/-</sup>*; ref. 17), C57BL/6 IL18-deficient mice (*Il18<sup>-/-</sup>*; ref. 18), C57BL/6 IL18 receptor alpha-deficient mice (*Il18Ra<sup>-/-</sup>*; ref. 19), C57BL/6 IL1 receptor-deficient mice (*Il1r<sup>-/-</sup>*; ref. 20), and C57BL/6 adenosine 2A receptor-deficient mice (*Adora2a<sup>-/-</sup>*; ref. 14) were bred in-house and maintained at the QIMR Berghofer Medical Research Institute. *Rag2<sup>-/-</sup>γc<sup>-/-</sup>* mice have been previously described (21). C57BL/6 *Ly2<sup>Cre/WT</sup> Cd39<sup>fl/fl</sup>* and *Cd335* (NCR1, NKp46)<sup>Cre/WT</sup> *Cd39<sup>fl/fl</sup>* mice were generated by crossing *Ly2ZCre* mice (from Dr. Irmgard Förster, University of Bonn, Germany; ref. 22) or *Cd335Cre* mice (from Eric Vivier; ref. 23), respectively, with *Cd39<sup>fl/fl</sup>* mice (obtained from the EUCOMM Consortium). Mouse strains were screened for genotype by PCR. Mice greater than 6 weeks of age were sex matched to the appropriate models. The number of mice in each treatment group or strain of mice for each experiment is indicated in the figure legends. In all studies, no mice were excluded based on preestablished criteria, and randomization was applied only immediately pretreatment in therapy experiments to ensure similar mean tumor size was the starting point. Experiments were conducted as approved by the QIMR Berghofer Medical Research Institute Animal Ethics Committee.

### Monoclonal antibody generation

The B66 antibody to mouse (m)CD39, and a D265A variant thereof, has been described previously (12). 617 and 619 monoclonal antibodies (mAb) are mouse IgG1 anti-mouse CD39 that have been previously described, and they do not inhibit CD39 ectoenzyme activity (12).

### Cell culture

Mouse B16F10 (melanoma) cells were grown in Dulbecco's Modified Eagle Medium supplemented with 10% fetal calf serum (FCS, Bovogen), 1% glutamine (Gibco), 1% HEPES (Gibco), and 1% penicillin/streptomycin (Gibco). Mouse LWT1 (melanoma), Renca (renal carcinoma), and 4T1.2 (mammary carcinoma) cells were cultured in RPMI-1640 supplemented with 10% FCS, 1% glutamine, and 1% penicillin/streptomycin (complete RPMI). All mouse tumors were CD39-negative in culture, as previously demonstrated (10). All cell lines were maintained at 37°C, 5% CO<sub>2</sub> and were not grown for more than 2 weeks of culture. Tumor cell injection and monitoring procedures were described in previous studies (10). All cell lines were routinely tested negative for *Mycoplasma*, but cell line authentication was not routinely performed.

### Bone marrow chimera construction

As previously described, CD45.1<sup>+</sup> *Ptprc<sup>a</sup>* WT mice and CD45.2<sup>+</sup> *Cd39<sup>-/-</sup>* recipient mice (9–10 mice per group) were irradiated (Gamma Cell) twice (4 hours apart) with a total dose of 1,050 cGy (21). Donor bone marrow (BM) cells (femur and tibia, 1 × 10<sup>7</sup>) from *Ptprc<sup>a</sup>* mice or *Cd39<sup>-/-</sup>* mice were then intravenously (i.v.) injected into the irradiated recipient mice to produce BM chimeric mice. Neomycin-containing water (1 mg/mL, Sigma-Aldrich N1876) was given to these

mice for 3 weeks. After confirming the BM reconstruction by flow cytometry on peripheral blood 8 weeks after BM cell injection, LWT1 cells (5 × 10<sup>5</sup>) were i.v. injected into the BM chimeric mice. Mice were then treated intraperitoneally (i.p.) with control immunoglobulin (cIg) or anti-CD39 as indicated below and in the figure legends. Lungs were harvested on day 14, and metastatic colonies on the surface of the lungs were counted using a dissecting microscope (6.7× magnification; Olympus SZ61, Olympus Life Sciences).

### Experimental and spontaneous tumor metastasis models

B16F10 melanoma (2 × 10<sup>5</sup>), LWT1 melanoma (5 × 10<sup>5</sup>), or Renca renal carcinoma (2 × 10<sup>5</sup>) cells were injected i.v. into the tail vein of mice. On days 0 and 3 after tumor inoculation, mice were treated i.p. with various doses of cIg (I-536, mIgG1; Leinco) or anti-CD39 (B66, mIgG1 or mIgG1 D265A) as indicated (from 5 to 200 μg per injection). Some groups of mice were treated with additional therapies alone or in combination with anti-CD39: POM1 (250 μg i.p. days 0, 1, 2, and 3; Santa Cruz Biotechnology); anti-PD-1 (RMP1-14, 250 μg i.p. days 0 and 3; Bio X Cell); anti-CD73 (2C5, mIgG1, 200 μg i.p. days 0 and 3; Tizona Therapeutics), anti-CD73 (TY/23, rat IgG2a, 200 μg i.p. days 0 and 3; Bio X Cell), A2AR inhibitor (A2ARi; SCH58261, 10 mg/kg i.p. on days 0 and 3; Sigma-Aldrich), IL2 (100,000 IU i.p. on days 0, 1, 2, and 3), or IL15/IL15Ra (0.5 μg/3 μg i.p. on days 0 and 3; R&D Systems), with schedules and doses as indicated in the figure legends. Lungs were harvested on day 14, and metastatic colonies on the surface of the lungs were counted using a dissecting microscope (as above).

For spontaneous metastasis and surgery, 2 × 10<sup>4</sup> 4T1.2 mammary carcinoma cells were injected into the fourth mammary fat pad as previously described (24). Mice were i.p. treated with cIg (200 μg), anti-CD39 (200 μg), anti-PD-1 (250 μg), or combination anti-CD39 and anti-PD-1 (200 μg and 250 μg, respectively) on days 14, 17, 20, and 24. The primary mammary gland tumor was resected on day 12. Mice were then monitored for survival as previously described (24).

### In vivo treatments and mechanism of action

In some groups of mice, depletion of NK cells or CD8<sup>+</sup> T cells or neutralization of IFNγ was performed by i.p. treatment on days –1, 0, and 7 with anti-asGM1 (rabbit Ig, 50 μg/mouse; Wako Pure Chemicals), anti-CD8β (rat IgG1, 53.5.8, 100 μg/mouse; Bio X Cell), or neutralizing anti-IFNγ (Armenian Hamster IgG, H22, 250 μg/mouse; Leinco Technologies). An appropriate isotype control was also used in these experiments. Clodronate-containing liposomes for the depletion of phagocytic cells and empty-control liposome preparations were used as described (clodrolip; sodium clodronate tetrahydrate, Farchemia SRL; ref. 25). Clodrolip and control liposomes were diluted in PBS and injected i.p. at 2 mg per 20 g body weight, 2 days prior to therapy. Subsequent doses of depleting and control liposome preparations (1 mg/20 g body weight) were administered on days 0, 2, and 4. Some groups of mice were neutralized for CD11b (5C6; Dr. Hideo Yagita, Juntendo University School of Medicine Tokyo, Japan, IL1β (B122; Leinco Technologies), or IL18 (SKII3AE4; kindly provided by Irmgard Förster, University of Bonn, Germany) or depleted of Ly6G<sup>+</sup> cells (1A8; Leinco) using the scheduling and dosing as indicated. These dosing schedules have previously been shown to functionally deplete or neutralize these cells and cytokines, respectively (12, 14, 25–29).

In some experiments, NK cells (CD45.2<sup>+</sup>CD3<sup>-</sup>NK1.1<sup>+</sup> using antibodies as below) were sorted from the spleens of WT or CD39<sup>-/-</sup> mice to 95% purity using a BD FACSAria III (BD Biosciences), and WT or CD39<sup>-/-</sup> NK cells (2 × 10<sup>5</sup>) were injected i.v. into *Rag2<sup>-/-</sup>γc<sup>-/-</sup>* mice. After 6 days, peripheral blood (retro-orbital) was collected to check

Yan et al.

the equivalent reconstitution of NK cells by flow cytometry. B16F10 ( $1 \times 10^5$ ) or LWT1 ( $1 \times 10^5$ ) melanoma cells were then injected i.v. into *Rag2<sup>-/-</sup>γc<sup>-/-</sup>* mice. Lungs were harvested on day 14, and metastatic colonies on the surface of the lungs were counted using a dissecting microscope.

### Flow cytometry

Single-cell suspensions from the lungs of tumor-bearing mice were prepared as previously described (30) and incubated for 20 minutes with anti-CD16/32 (2.4G2, hybridoma in house) to block nonspecific Fc binding. Cells then were surface stained for 20 minutes with antibody cocktails on ice. The following antibodies were used for flow cytometry analyses: anti-CD45.2 (clone 104), anti-TCRβ (clone H57-597), anti-NK1.1 (clone PK136), anti-NKp46 (clone 29A1.4), anti-CD27 (clone LG.7F9), anti-MHC II (clone M5/114.15.2), anti-CD4 (clone GK1.5), and anti-FOXP3 (clone JFK-16S; all from eBioscience); anti-DNAM-1 (clone 480.1), anti-CD11b (clone M1/70), anti-Ly6G (clone 1A8), anti-CD64 (clone X54-5/7.1), anti-P2X7 (clone 1F11), anti-CD24 (clone M1/69), anti-Ly6C (clone HK1.4), anti-CD39 (clone Duha59, 24DMS1), anti-CD11c (clone N418), anti-CD19 (clone 6D5), anti-CD8α (clone 53-6.7), and anti-CD3 (clone 17A2; all from BioLegend). The Zombie Aqua Fixable Viability Kit (BioLegend) was used to exclude the dead cells. The FoxP3 fixation/permeabilization kit from eBioscience was used for FOXP3 staining. For intracellular cytokine staining, cells were surface stained as described above and then fixed and permeabilized with a cytofix/cytoperm kit (BD Biosciences) followed by staining with anti-IFNγ (clone XMG1.2) or isotype (clone eBio299Arm) antibody (both from BioLegend). All data were collected on a Fortessa 4 flow cytometer (BD Biosciences) and analyzed with FlowJo v10 software (TreeStar, Inc.).

### Ex vivo NK cell cytokine and degranulation assay

Lung single-cell suspensions were incubated in complete RPMI-1640 media containing cell stimulation cocktail [PMA (40.5 nmol/L)/ionomycin (669.3 nmol/L)] plus protein transport inhibitors (GolgiStop and GolgiPlug; 1/1,000 dilution) for 3 hours. Cells were then stained, as indicated above, for surface markers and intracellular cytokine production. A CD107a staining assay was used to assess the degranulation status of NK cells. Briefly, anti-CD107a (clone 1D4B, BioLegend) was added to single-cell suspensions during the stimulation period before the cells were surface stained and analyzed by flow cytometry.

### Statistical analysis

Statistical analysis was determined with GraphPad Prism 7 (GraphPad Software). A one-tailed Mann-Whitney *U* test was used for comparisons of two groups. Significance of differences was also calculated by the log-rank *t* test for Kaplan-Meier survival analysis or one-way ANOVA as necessary. Tukey multiple comparison tests were utilized unless otherwise indicated. Differences between groups are shown as the mean ± SEM. *P* values of less than 0.05 were considered statistically significant.

## Results

### Antimetastatic efficacy of an anti-mouse CD39

To examine the antimetastatic efficacy of targeting CD39 using a mouse mAb (clone B66) that allosterically inhibits the mouse ectoenzyme CD39 (12), we used two experimental metastasis models of mouse melanoma and one model of renal carcinoma. The first, LWT1, is a metastatic variant of the *Braf<sup>V600E</sup>*-mutant

SM1WT1 melanoma, whose metastatic seeding is controlled by host NK cells (31, 32). We first demonstrated that at days 0 (tumor inoculation) and 3, injection of anti-CD39 (200 μg) was effective in suppressing LWT1 lung metastases (Fig. 1A). A titration of anti-CD39 was used to determine optimal dosing in the same model (Fig. 1B). Maximal response was observed at doses of 100 to 200 μg, with doses as little as 50 μg still able to statistically reduce LWT1 lung metastases. In a second model, B16F10, a melanoma that has been used for numerous studies of NK cell-mediated control of metastasis (30, 33), anti-CD39 was also effective in reducing metastatic burden in the lungs (Fig. 1C). When dosed at the optimal concentration, targeting CD39 with an enzymatic antibody inhibitor was more efficacious than the CD39 small-molecule inhibitor POM1 or targeting other molecules in the ATP/adenosine axis, including an A2ARi (SCH58261) and two different anti-CD73 antibodies. Similarly, anti-PD-1 treatment was also suboptimal at reducing metastatic burden (Fig. 1D). In the Renca model of experimental renal carcinoma metastasis, anti-CD39 reduced metastases and was also more effective than POM1 (Fig. 1E). Fc engagement was not required for antimetastatic efficacy, as a variant of anti-CD39 with a mIgG1 isotype featuring an additional Fc mutation to further diminish any Fc receptor interactions (D265A) was as active as the WT mIgG1 isotype (Fig. 1F). The ability to block CD39 ectoenzyme activity, rather than merely binding to the antigen, was critical to the observed efficacy, as two other CD39-targeting mAbs (Tz-617; Tz-619) lacking enzymatic inhibition with comparable affinity to B66 did not affect LWT1 (Fig. 1G) or B16F10 lung metastasis formation (Fig. 1H). The antimetastatic effect of anti-CD39 (B66) in WT mice was greater than the reduction in lung metastases observed in *Cd39<sup>-/-</sup>* or *Cd73<sup>-/-</sup>* mice (Supplementary Fig. S1). This result suggests that compensatory mechanisms or receptor desensitization may partially account for the loss of CD39 in the *Cd39<sup>-/-</sup>* mice.

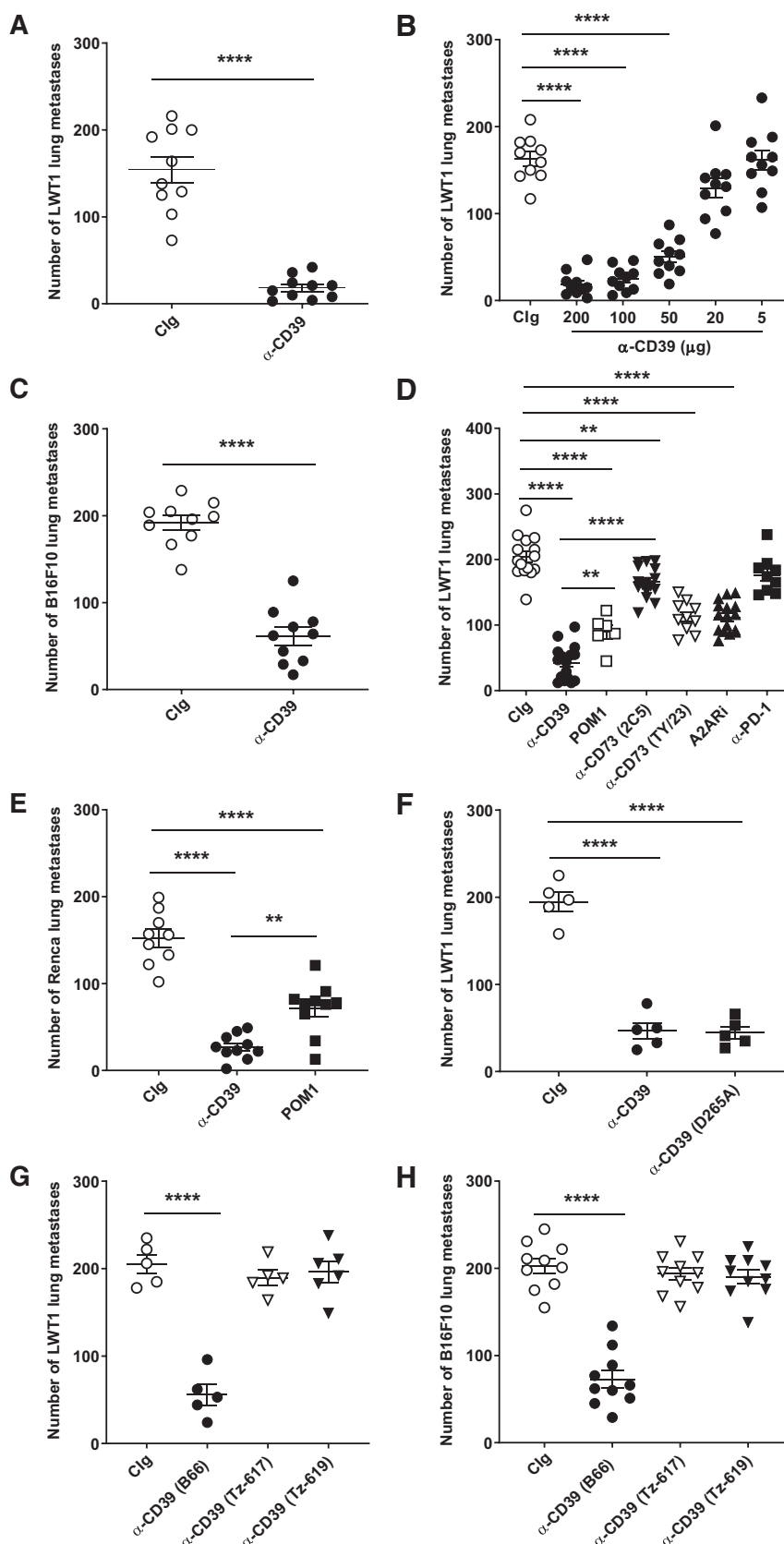
### The role of NK cells and host CD39 in the antimetastatic activity of anti-CD39

We next assessed the mechanism by which lung metastases were reduced in the anti-CD39-treated mice. Using the LWT1 melanoma model, the antimetastatic effect of CD39 enzymatic inhibition was completely abrogated in *RAG2<sup>-/-</sup>γc<sup>-/-</sup>* mice that lack all lymphocytes (Fig. 2A). Follow-up experiments using specific depletion of NK cells or CD8<sup>+</sup> T cells or neutralization of IFNγ revealed that NK cells and IFNγ, but not CD8<sup>+</sup> T effector cells, were required for anti-CD39 control of experimental lung metastases (Fig. 2B). Using *Cd39<sup>-/-</sup>* mice, it was clear that host CD39 expression was also needed for anti-CD39 reduction of both LWT1 (Fig. 2C) and B16F10 (Fig. 2D) lung metastases.

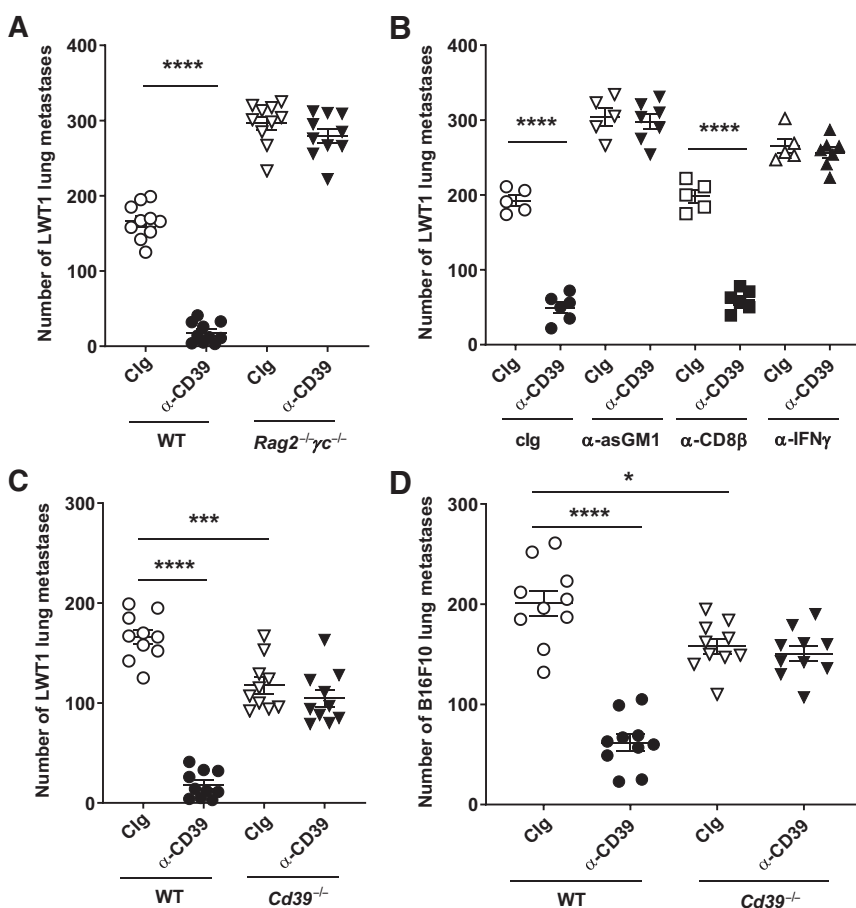
To examine the mechanism of anti-CD39 in NK cell control of experimental lung tumor metastasis, lung mononuclear cells were harvested from mice 1 and 3 days after tumor inoculation and a single dose of anti-CD39. After 3 days, an increase in the percentage of IFNγ-producing NK cells and in IFNγ mean fluorescence intensity (MFI) in NK cells following anti-CD39 treatment was seen compared with cIg (Fig. 3A). Degranulation by NK cells, measured by CD107a, was also increased, but changes were observed as early as 1 day after anti-CD39 therapy (Fig. 3B). The percentage and number of leukocytes (CD45.2<sup>+</sup>; Supplementary Fig. S2A) and NK cells (Supplementary Fig. S2B) was not increased by anti-CD39 treatment, nor was any modulation in maturation seen, defined by the number and proportion of DNAM-1<sup>+</sup> NK cells (ref. 34; Supplementary Fig. S2C). Additional assessment of NK cell differentiation using previously described CD27 and CD11b staining (35) also did not reveal any significant changes

**Figure 1.**

Targeting CD39 suppresses experimental lung metastases. **A**, Groups ( $n = 10/\text{group}$ ) of B6 WT mice were injected i.v. with LWT1 ( $5 \times 10^5$ ) melanoma cells on day 0 and treated i.p. with clg (200  $\mu\text{g}$ ) or anti-CD39 (200  $\mu\text{g}$ ) on days -1, 0, and 3. **B**, Groups ( $n = 10/\text{group}$ ) of B6 WT mice were injected i.v. with LWT1 ( $5 \times 10^5$ ) melanoma cells on day 0 and treated i.p. with clg (200  $\mu\text{g}$ ) or anti-CD39 at the concentrations indicated on days 0 and 3. **C**, Groups ( $n = 10/\text{group}$ ) of B6 WT mice were injected i.v. with B16F10 ( $2 \times 10^5$ ) cells on day 0 and treated i.p. with clg (200  $\mu\text{g}$ ) or anti-CD39 (200  $\mu\text{g}$ ) on days 0 and 3. **D**, Groups ( $n = 6-16/\text{group}$ ) of B6 WT mice were injected i.v. with LWT1 ( $5 \times 10^5$ ) melanoma cells on day 0 and treated i.p. with clg (200  $\mu\text{g}$ ), anti-CD39 (200  $\mu\text{g}$ ), A2ARi (SCH58261; 10 mg/kg), anti-CD73 (TY/23 or 2C5; 200  $\mu\text{g}$ ), or anti-PD-1 (250  $\mu\text{g}$  i.p.) on days 0 and 3 or POM1 (250  $\mu\text{g}$  i.p.) on days 0, 1, 2, and 3. Pooled from two experiments. **E**, Groups ( $n = 9-10/\text{group}$ ) of BALB/c WT mice were injected i.v. with  $2 \times 10^5$  Renca cells on day 0 and treated i.p. with clg (200  $\mu\text{g}$ ) or anti-CD39 (200  $\mu\text{g}$ ) on days 0 and 3 or POM1 (250  $\mu\text{g}$  i.p.) on days 0, 1, 2, and 3. **F**, Groups ( $n = 5/\text{group}$ ) of B6 WT mice were injected i.v. with LWT1 ( $5 \times 10^5$ ) melanoma cells on day 0 and treated i.p. with clg (200  $\mu\text{g}$ ) or anti-CD39 (B66 or B66D265A; 200  $\mu\text{g}$  each) on days 0 and 3. **G**, Groups ( $n = 5-6/\text{group}$ ) of B6 WT mice were injected i.v. with LWT1 ( $5 \times 10^5$ ) cells on day 0 and treated i.p. with clg (200  $\mu\text{g}$ ) or various anti-CD39 (200  $\mu\text{g}$ ) on days 0 and 3 as indicated. **H**, Groups ( $n = 10/\text{group}$ ) of B6 WT mice were injected i.v. with B16F10 ( $2 \times 10^5$ ) cells on day 0 and treated i.p. with clg (200  $\mu\text{g}$ ) or various anti-CD39 (200  $\mu\text{g}$ ) on days 0 and 3 as indicated. The lungs were harvested on day 14, and the metastatic burden was quantified by counting colonies on the lung surface under a microscope. Mean  $\pm$  SEM are shown. Experiments were performed once unless indicated. Significant differences among various treatment groups were determined by one-way ANOVA, followed by the Tukey multiple comparison test (\*\*,  $P < 0.01$ ; \*\*\*\*,  $P < 0.0001$ ).



Yan et al.

**Figure 2.**

Anti-CD39's antimetastatic efficacy is dependent on NK cells and host IFN $\gamma$  and CD39. **A**, Groups ( $n = 10$ /group) of B6 WT and Rag2 $^{-/-}$  $\gamma$ c $^{-/-}$  mice were injected i.v. with LWT1 ( $5 \times 10^5$ ) melanoma cells on day 0 and treated i.p. with clg (200  $\mu$ g) or anti-CD39 (200  $\mu$ g) on days 0 and 3. **B**, Groups ( $n = 5-7$ /group) of B6 WT mice were injected i.v. with LWT1 ( $5 \times 10^5$ ) melanoma cells on day 0 and treated i.p. clg (200  $\mu$ g) or anti-CD39 (200  $\mu$ g) on days 0 and 3 and anti-asGM1 (50  $\mu$ g), anti-CD8 $\beta$  (100  $\mu$ g), anti-mIFN $\gamma$  (250  $\mu$ g), or clg (100  $\mu$ g) on days -1, 0, and 7. **C**, Groups ( $n = 10$ /group) of B6 WT and CD39 $^{-/-}$  mice were injected i.v. with  $5 \times 10^5$  LWT1 melanoma cells on day 0 and treated i.p. with clg (200  $\mu$ g) or anti-CD39 (200  $\mu$ g) on days 0 and 3. **D**, Groups ( $n = 10$ /group) of B6 WT mice and CD39 $^{-/-}$  mice were injected i.v. with B16F10 ( $2 \times 10^5$ ) cells on day 0 and treated i.p. with clg (200  $\mu$ g) or anti-CD39 (200  $\mu$ g) on days 0 and 3. The metastatic burden was quantified in the lungs after 14 days by counting colonies on the lung surface. Mean  $\pm$  SEM are shown. Experiments were performed once unless indicated. Significant differences among various treatment groups were determined by one-way ANOVA, followed by the Tukey multiple comparison test (\*,  $P < 0.05$ ; \*\*\*,  $P < 0.001$ ; \*\*\*\*,  $P < 0.0001$ ).

post anti-CD39 therapy (Supplementary Fig. S2D–S2F). We were only able to detect minimal expression of P2X7 on NK cells in the lungs, and this was not altered by anti-CD39 (Supplementary Fig. S3). Thus, the major impact of anti-CD39 treatments appeared to be a gain of NK cell effector function, rather than infiltration or proliferation. Assessment of the myeloid cells and granulocytes post anti-CD39 revealed a specific reduction in alveolar macrophages (Fig. 3C–G), which correlated with the coexpression of CD39 and P2X7 (eATP receptor) displayed by these cells in LWT1 tumor-burdened lungs (Fig. 3H; Supplementary Fig. S4).

#### Role of P2X7–NALP3–IL18 inflammasome in anti-CD39 antimetastatic activity

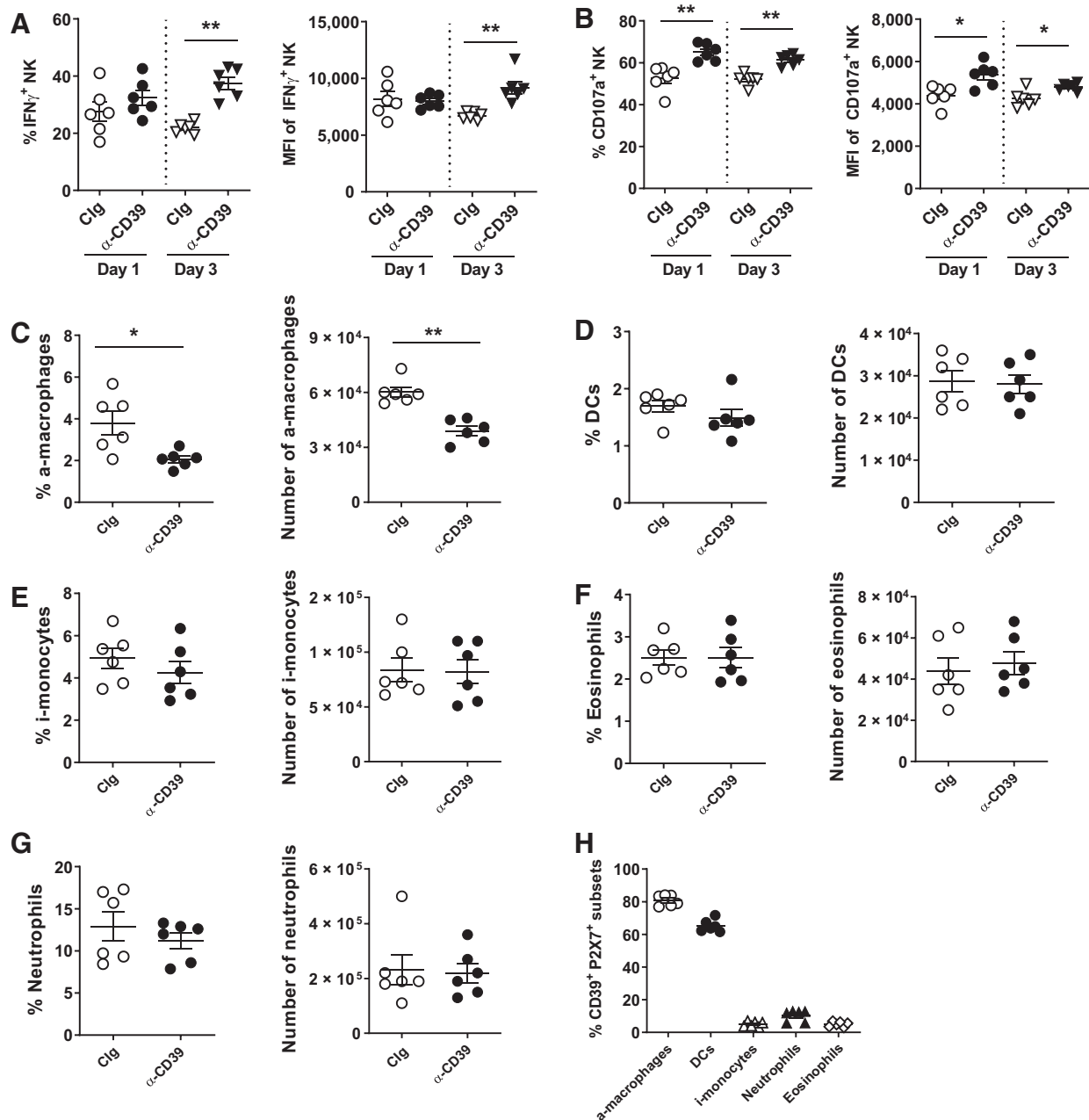
CD39 is the pivotal regulator balancing proinflammatory ATP and immunosuppressive adenosine within the TME. P2X7 is one of the major functional eATP receptors on immune cells and is a critical factor in NALP3 inflammasome activity (36). Given this, we next examined whether host P2X7 receptor and downstream inflammasome components contributed to the antimetastatic activity of anti-CD39 (Fig. 4). In the LWT1 model, anti-CD39 effectively reduced metastases in WT mice but was ineffective in Cd39 $^{-/-}$  (as shown above), Pycard $^{-/-}$  (ASC-deficient), Nalp3 $^{-/-}$ , and P2rx7 $^{-/-}$  mice (Fig. 4A; Supplementary Fig. S5). Similarly, in the B16F10 lung metastasis model, anti-CD39 was ineffective in Nalp3 $^{-/-}$  and P2rx7 $^{-/-}$  mice (Fig. 4B). The A2ARi (SCH58261) still mediated antimetastatic effects in these strains compared with WT mice (Fig. 4B; Supplementary Fig. S5), suggesting that in this setting,

adenosine-mediated immune suppression was partially enabling metastasis spread, but the effects of anti-CD39 treatment required a functional inflammasome. As previously described (37, 38), P2rx7 $^{-/-}$  mice displayed more lung metastases than WT mice in both LWT1 and B16F10 models, whereas metastasis was lower in Pycard $^{-/-}$  and Nalp3 $^{-/-}$  mice (Fig. 4A and B; Supplementary Fig. S5). These data implicated the P2X7–ASC–NALP3 inflammasome axis in the antimetastatic activity of anti-CD39 and suggest a mechanism of action involving the maintenance of proinflammatory ATP, as opposed to simply impacting the downstream triggering of A2AR by adenosine.

Given that the P2X7 receptor was coexpressed by CD39-expressing myeloid cells and that macrophages were reduced in the tumor-bearing lungs of anti-CD39-treated mice, we next assessed the importance of myeloid cells on the antimetastatic activity of anti-CD39 using two approaches. First, myeloid cells were depleted using clodronate liposomes. Second, myeloid cell movement was prevented using anti-CD11b (Fig. 4C and D). Basal LWT1 metastasis was reduced under these conditions, and we observed suboptimal anti-CD39 activity when myeloid cells were depleted or immobilized. By contrast, additional experiments to deplete Ly6G $^{+}$  neutrophils had no significant impact on anti-CD39 antitumor activity (Fig. 4D). These data were consistent with a role for myeloid cell P2X7–NALP3 inflammasome because, although macrophages were reduced post anti-CD39, myeloid cells were required for the activity of anti-CD39.

ATP-dependent NALP3 inflammasome activation in macrophages is known to elicit lymphocyte effector responses via the activation and secretion of IL1 and IL18 cytokines (39, 40). Thus, we next investigated

## New Mechanism of Anti-CD39 Control of Metastases

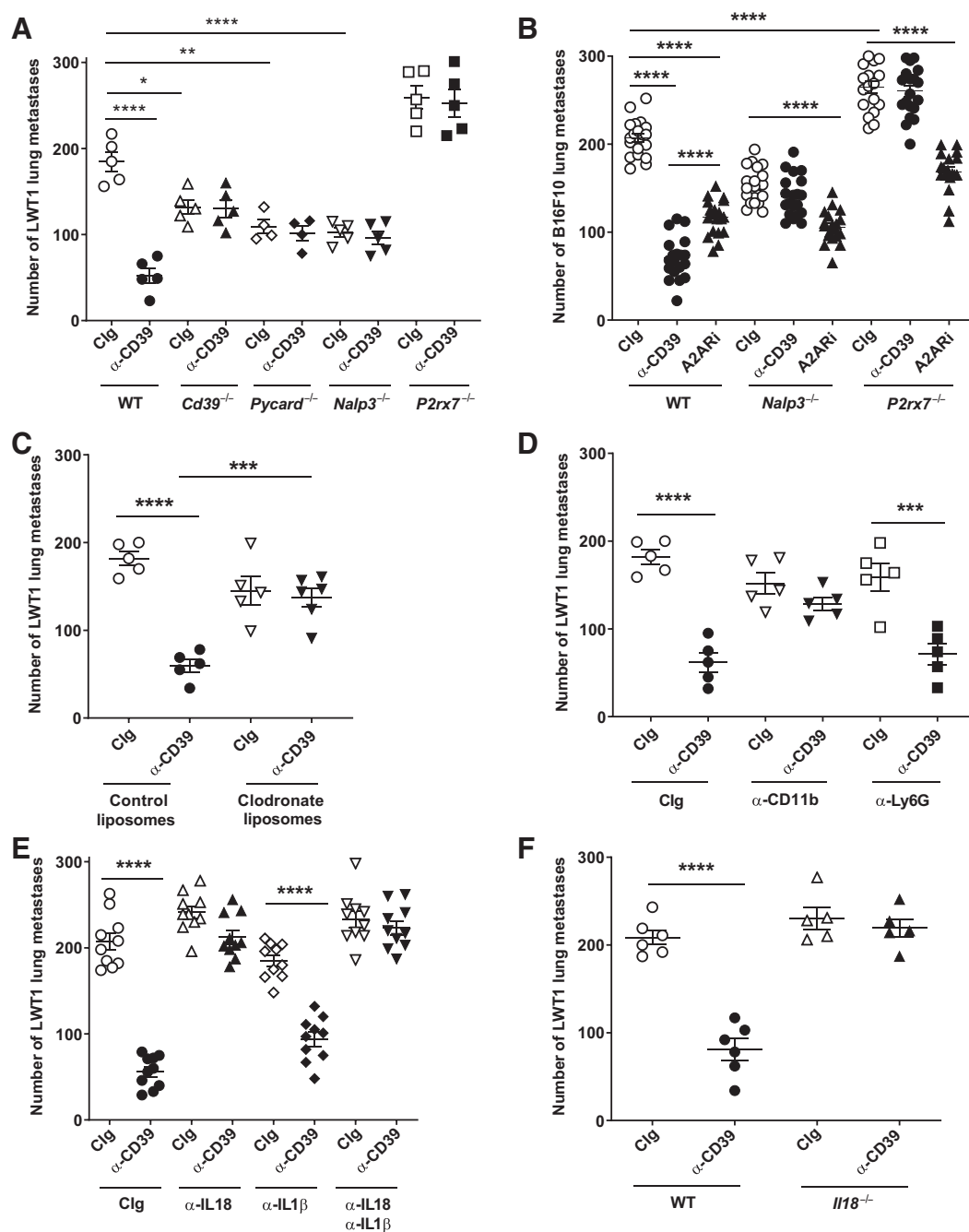
**Figure 3.**

Anti-CD39 enhances the effector function of NK cells *in vivo*. Groups ( $n = 6$ /group) of B6 WT mice were injected i.v. with LWT1 ( $5 \times 10^5$ ) melanoma cells on day 0 and treated i.p. with clg (200  $\mu$ g) or anti-CD39 (200  $\mu$ g) on day 0. The lungs were harvested on days 1 and 3 after tumor inoculation, and single-cell suspensions were prepared for flow-cytometric analyses. Summary graphs showing the percentage and MFI of various IFN $\gamma$ -producing (A) and CD107a<sup>+</sup> (B) NK cells are provided. C-H, Mice were i.v. injected with  $5 \times 10^5$  LWT1 cells and i.p. treated with clg or anti-CD39 (200  $\mu$ g) on day 0. Lung single-cell suspensions were generated on day 1 relative to tumor cell inoculation. C-G, The proportions and number of various myeloid and granulocytes, including alveolar macrophages (a-macrophages). H, The proportion of double-positive CD39<sup>+</sup>P2X7<sup>+</sup> myeloid cells and granulocytes, defined as a-macrophages (Ly6G<sup>-</sup>CD64<sup>+</sup>CD24<sup>-</sup>CD11c<sup>+</sup>CD11b<sup>-</sup>CD45.2<sup>+</sup>), dendritic cells (DC; Ly6G<sup>-</sup>CD64<sup>-</sup>MHCII<sup>+</sup>CD11c<sup>+</sup>CD45.2<sup>+</sup>), inflammatory monocytes (i-monocytes; Ly6G<sup>-</sup>MHCII<sup>lo</sup>CD11b<sup>+</sup>CD64<sup>+</sup>Ly6C<sup>+</sup>CD11c<sup>-</sup>CD45.2<sup>+</sup>), neutrophils (Ly6G<sup>+</sup>CD11c<sup>-</sup>CD45.2<sup>+</sup> cells), and eosinophils (Ly6G<sup>-</sup>CD64<sup>-</sup>MHCII<sup>-</sup>CD11b<sup>+</sup>CD45.2<sup>+</sup>). Mean  $\pm$  SEM from one experiment are shown. Significant differences between the populations were determined by the Mann-Whitney *U* test (\*,  $P < 0.05$ ; \*\*,  $P < 0.01$ ).

the role of these cytokines on the antimetastatic activity of anti-CD39. When IL18 was blocked with or without IL1 $\beta$  blockade, treatment with anti-CD39 failed to elicit an antimetastatic effect, whereas neutralization of IL1 $\beta$  alone had no significant impact on anti-CD39 treatment

(Fig. 4E). This suggested that the antimetastatic effects of IL18 were specific to the mechanism of action of CD39 ectoenzyme inhibition, rather than a broad measure of inflammasome activation. These data were supported by the inability of *Il18*<sup>-/-</sup> mice to control LWT1

Yan et al.

**Figure 4.**

Antimetastatic activity of anti-CD39 is dependent on the P2X7-NALP3 inflammasome and IL18. **A**, Groups ( $n = 4$ -5/group) of B6 WT, *Cd39*<sup>-/-</sup>, *Pycard*<sup>-/-</sup>, *Nalp3*<sup>-/-</sup>, and *P2rx7*<sup>-/-</sup> mice were injected i.v. with LWT1 ( $5 \times 10^5$ ) melanoma cells day 0 and treated i.p. with clg (200  $\mu$ g) or anti-CD39 (200  $\mu$ g) on days 0 and 3. **B**, Groups ( $n = 18$ -20/group) of B6 WT mice, *Nalp3*<sup>-/-</sup>, and *P2rx7*<sup>-/-</sup> mice were injected i.v. with B16F10 ( $2 \times 10^5$ ) melanoma cells on day 0 and treated i.p. with clg (200  $\mu$ g), anti-CD39 (200  $\mu$ g), or A2ARi (SCH58261; 10 mg/kg) on days 0 and 3. Pool of three experiments performed. **C**, Groups ( $n = 5$ -6/group) of WT mice were injected i.v. with LWT1 ( $5 \times 10^5$ ) melanoma cells on day 0 and treated i.p. with anti-CD39 (200  $\mu$ g) or clg (200  $\mu$ g) on days 0 and 3. Mice additionally received either clodronate or control liposomes on days -2 (2 mg/20 g mouse), 0 (1 mg/20 g mouse thereafter), 2, and 4. **D**, Groups ( $n = 5$ /group) of WT mice were injected i.v. with LWT1 ( $5 \times 10^5$ ) melanoma cells on day 0 and treated i.p. with anti-CD39 (200  $\mu$ g) or clg (200  $\mu$ g) on days 0 and 3. Mice also received either clg, anti-CD11b, or anti-Ly6G (250  $\mu$ g i.p.) on days -1, 0, and 3. **E**, Groups ( $n = 5$ /group) of B6 WT mice were injected i.v. with LWT1 ( $5 \times 10^5$ ) melanoma cells on day 0 and treated i.p. with anti-CD39 (200  $\mu$ g) or clg (200  $\mu$ g) on days 0 and 3. Mice also received either clg, anti-IL18, anti-IL1 $\beta$ , or both (250  $\mu$ g i.p. each) on days -1, 0, 3, and 9 or days -1, 0, and 7 (two experiments pooled). **F**, Groups ( $n = 5$ /group) of B6 WT or B6 *Il18*<sup>-/-</sup> mice were injected i.v. with LWT1 ( $5 \times 10^5$ ) melanoma cells on day 0 and treated i.p. with clg (200  $\mu$ g) or anti-CD39 (200  $\mu$ g) on days 0 and 3. The metastatic burden was quantified in the lungs after 14 days by counting colonies on the lung surface. Mean  $\pm$  SEM are shown. Significant differences among various treatment groups were determined by one-way ANOVA, followed by the Tukey multiple comparison test (\*,  $P < 0.05$ ; \*\*,  $P < 0.01$ ; \*\*\*,  $P < 0.001$ ; \*\*\*\*,  $P < 0.0001$ ).

metastasis (Fig. 4F), and *III18<sup>-/-</sup>* and *III18Ra<sup>-/-</sup>* mice to control B16F10 metastasis (Supplementary Fig. S6) when treated with anti-CD39 in contrast to WT or *III1R<sup>-/-</sup>* mice, both of which had significantly reduced metastatic burden when treated with anti-CD39.

### Role of myeloid CD39 in anti-CD39-mediated control of metastases

Given the importance of host CD39 in the antimetastatic activity of anti-CD39, we next determined the role of hematopoietic and non-hematopoietic sources of CD39 using WT/*Cd39<sup>-/-</sup>* BM chimeras. The results demonstrated that anti-CD39 efficacy was dependent on the presence of functional CD39 on the donor BM (*Ptprc<sup>a</sup>*) rather than the recipient mice (Fig. 5A; Supplementary Fig. S7). This indicated hematopoietic CD39 expression was essential and was consistent with CD39 expression on lung-infiltrating immune cells, including infil-

trating NK cells, following LTW1 and B16F10 tumor inoculation and previously reported efficacy post treatment with POM1 (10). We next examined the possible role of NK cell CD39 in the antimetastatic activity of anti-CD39. Sorted, purified WT or *Cd39<sup>-/-</sup>* NK cells were transferred into lymphocyte-deficient *Rag2<sup>-/-</sup> $\gamma$ c<sup>-/-</sup>* recipients, and after 6 days, both sets of recipients had reconstituted equivalently with donor NK cells (Supplementary Fig. S7). Challenge of these mice and nontransferred *Rag2<sup>-/-</sup> $\gamma$ c<sup>-/-</sup>* recipients with LWT1 (Fig. 5B) or B16F10 (Fig. 5C) melanoma cells demonstrated that both WT and *Cd39<sup>-/-</sup>* NK cells were capable of offering some protection from lung metastases. Anti-CD39 remained effective in both sets of mice that received NK cells but was ineffective in nontransferred recipients (Fig. 5B and C).

To further assess whether myeloid cells and/or NK cell CD39 expression was important in the antimetastatic activity of anti-CD39,

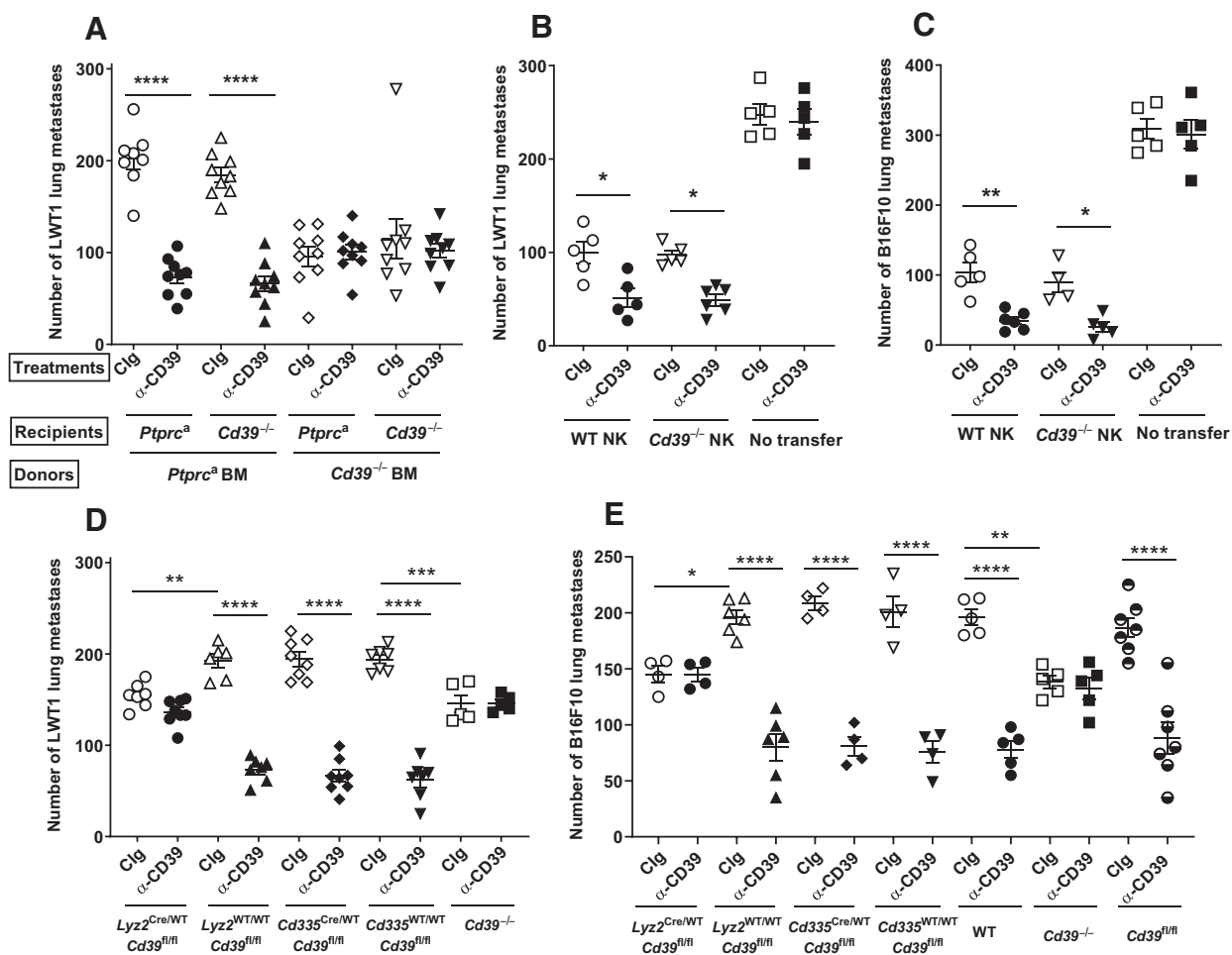


**Figure 5.**

Role of hematopoietic, but not NK cell, CD39 in antimetastatic activity of anti-CD39. **A**, Indicated groups ( $n = 8-9$ /group) of BM chimeric mice were injected i.v. with LWT1 ( $5 \times 10^5$ ) melanoma cells on day 0 and treated with clg (200  $\mu$ g) or anti-CD39 (200  $\mu$ g) on days 0 and 3. **B** and **C**, B6 WT or *Cd39<sup>-/-</sup>* NK cells ( $2 \times 10^5$ ) were injected i.v. into *Rag2<sup>-/-</sup> $\gamma$ c<sup>-/-</sup>* mice. One group did not receive NK cells. After 6 days, blood was collected to check the equivalent reconstitution of NK cells by flow cytometry. LWT1 ( $1 \times 10^5$ ; **B**) or B16F10 ( $1 \times 10^5$ ; **C**) melanoma cells were injected i.v. into *Rag2<sup>-/-</sup> $\gamma$ c<sup>-/-</sup>* mice. **D**, Groups ( $n = 5-8$ /group) of B6 *Lyz2<sup>Cre/WT</sup> Cd39<sup>fl/fl</sup>*, *Lyz2<sup>WT/WT</sup> Cd39<sup>fl/fl</sup>*, *Cd335<sup>Cre/WT</sup> Cd39<sup>fl/fl</sup>*, *Cd335<sup>WT/WT</sup> Cd39<sup>fl/fl</sup>*, and *Cd39<sup>-/-</sup>* mice were injected i.v. with LWT1 ( $5 \times 10^5$ ) melanoma cells on day 0 and treated i.p. with clg (200  $\mu$ g) or anti-CD39 (200  $\mu$ g) on days 0 and 3. Pool of two experiments performed. **E**, Groups ( $n = 4-7$ /group) of B6 *Lyz2<sup>Cre/WT</sup> Cd39<sup>fl/fl</sup>*, *Lyz2<sup>WT/WT</sup> Cd39<sup>fl/fl</sup>*, *Cd335<sup>Cre/WT</sup> Cd39<sup>fl/fl</sup>*, *Cd335<sup>WT/WT</sup> Cd39<sup>fl/fl</sup>*, WT, *Cd39<sup>-/-</sup>*, and *Cd39<sup>fl/fl</sup>* mice were injected i.v. with B16F10 ( $2 \times 10^5$ ) melanoma cells on day 0 and treated i.p. with clg (200  $\mu$ g) or anti-CD39 (200  $\mu$ g) on days 0 and 3. Pool of two experiments performed. Lungs were harvested on day 14, and metastatic colonies on the surface of the lungs were counted using a dissecting microscope. Mean  $\pm$  SEM are shown. Significant differences among various treatment groups were determined by one-way ANOVA, followed by the Tukey multiple comparison test (\*,  $P < 0.05$ ; \*\*,  $P < 0.01$ ; \*\*\*,  $P < 0.001$ ; \*\*\*\*,  $P < 0.0001$ ).

we created conditional strains where CD39 was deleted in myeloid (*Lyz2Cre*) or NK (*Cd335(NCR1)Cre*) cells (Supplementary Figs. S8–S9) in the LWT1 and B16F10 models, and revealed two findings (Fig. 5D and E). First, basal metastasis (cIg-treated) was reduced in *Lyz2<sup>Cre/WT</sup> Cd39<sup>fl/fl</sup>* mice in a similar manner to global *Cd39<sup>-/-</sup>* mice. In contrast, *Lyz2<sup>WT/WT</sup> Cd39<sup>fl/fl</sup>* mice, *Cd335<sup>WT/WT</sup> Cd39<sup>fl/fl</sup>* mice, and *Cd335<sup>Cre/WT</sup> Cd39<sup>fl/fl</sup>* mice displayed a similar higher basal metastasis. Second, anti-CD39 was only effective in these later strains and suppressed metastasis whether or not Cd39 was deleted from NK cells (Fig. 5D and E). However, anti-CD39 was not effective in mice with Cd39 deleted in myeloid cells (*Lyz2Cre* strain) or globally (*Cd39<sup>-/-</sup>*). Collectively, these data showed that NK cell expression of CD39 was dispensable for the antimetastatic activity of anti-CD39. Rather, myeloid cells and their expression of CD39 was necessary for both CD39 and anti-CD39-mediated control of metastases in these two models.

### Spontaneous metastasis and combinations

To examine the potential therapeutic effect of anti-CD39 on a spontaneous metastasis model, we used the orthotopic 4T1.2 mammary carcinoma model where immunotherapy was administered following (adjuvant) surgical resection of the primary tumor. In this model, mice left untreated or treated with cIg alone typically succumb to metastatic burden in the lung, bones, and other organs within 35 to 50 days of surgery. Survival of mice was monitored following adjuvant immunotherapy post-surgery (Fig. 6). The anti-CD39 and anti-PD-1 combination was more effective at improving survival than either monotherapy alone.

Finally, given the strong antimetastatic activity of anti-CD39 in several models of lung metastases, including in combination with anti-PD-1 therapy, we then examined anti-CD39 in combination with therapies that specifically enhance NK cell function, including IL2 and IL15 and an A2ARi, SCH58261. Both IL2 and IL15 were effective monotherapies against experimental lung metastases, but the combi-

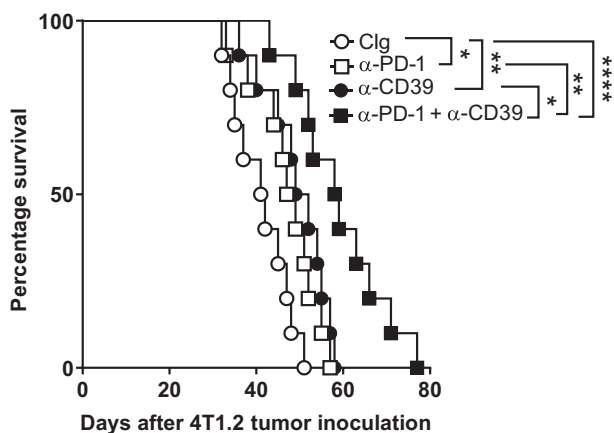


**Figure 6.**

Adjuvant treatment with combination anti-CD39 and anti-PD-1 enhances survival from spontaneous tumor metastases. Groups ( $n = 10/\text{group}$ ) of BALB/c WT mice were injected with 4T1.2 ( $2 \times 10^4$ ) cells in the mammary fat pad on day 0. The tumor was surgically resected on day 12, and mice were treated i.p. with cIg (200  $\mu\text{g}$ ), anti-CD39 (200  $\mu\text{g}$ ), anti-PD-1 (250  $\mu\text{g}$ ), or combination of anti-CD39 and anti-PD-1 (200  $\mu\text{g}$ ; 250  $\mu\text{g}$ ) on days 14, 17, 20, and 24. The Kaplan-Meier curves for overall survival of each group are shown. Significant differences between the indicated groups were determined by the log-rank test (\*,  $P < 0.05$ ; \*\*,  $P < 0.01$ ; \*\*\*,  $P < 0.0001$ ).

nation with anti-CD39 was even more effective (Fig. 7A and B). Despite the fact that blockade of extracellular adenosine generation may occur by anti-CD39 preventing ATP hydrolysis into AMP and subsequently adenosine via CD73, a combinatorial effect on antimetastatic activity was observed between anti-CD39 and the A2ARi (SCH58261) over either monotherapy alone (Fig. 7C). Further supporting this finding was the observed antimetastatic efficacy of anti-CD39 treatment in *Adora2a<sup>-/-</sup>* mice (Supplementary Fig. S10). This highlights the potential of targeting more than one molecule in the adenosinergic pathway and raises the possibility that other sources of adenosine may contribute to the generation of an immunosuppressive TME (41).

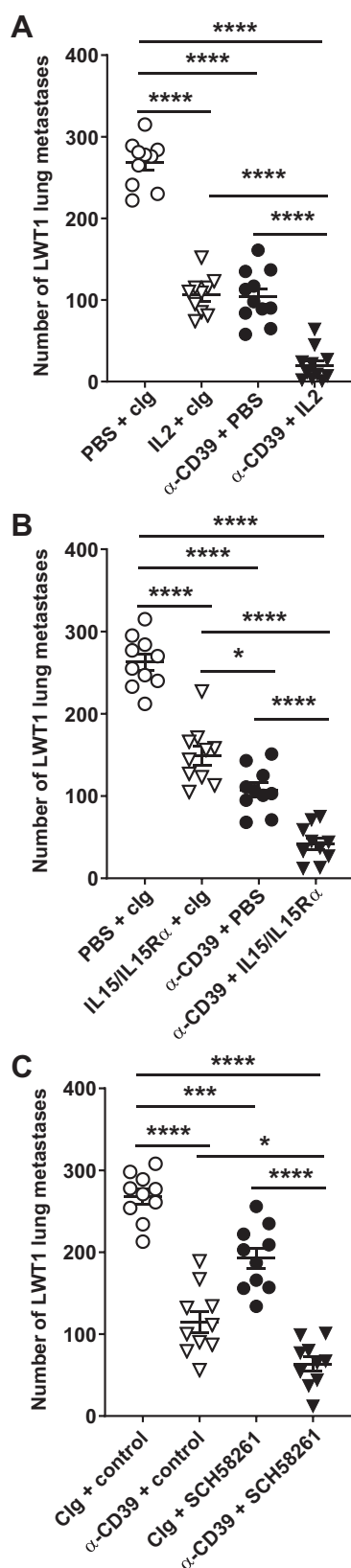
## Discussion

Although there has been a lot of interest in the impact of the adenosine pathway on T-cell effector function in tumors, very little focus has been applied to the role of this pathway in innate control of metastatic disease. Here, we described the antimetastatic efficacy and the mechanism of action of a mouse CD39-specific mAb. As previously reported (10, 42), immune surveillance of metastatic spread in these models is driven by NK cell-mediated and IFN $\gamma$ -dependent processes, so it is expected that enzymatic inhibition of CD39 mediates antimetastatic effects via these mechanisms. Because CD39 is inducible under inflammatory conditions, both on a number of tumors (43–45) and immune cell populations, and because T regulatory cells and myeloid cells constitutively express CD39, it was of critical importance to delineate that the observed antimetastatic efficacy of anti-CD39 treatment requires inhibition of ATPase activity and is independent of any Fc receptor engagements. Although we found hallmarks of NK cell activation in the lungs, the overall number, frequency, and differentiation state of NK cells were not affected.

Antibody-mediated inhibition of CD39 appeared to be superior to agents targeting the ATP/adenosine axis, as well as the CD39 small-molecule inhibitor POM1 that has previously been used *in vivo* (10). Superiority over POM1 can be attributed to multiple factors, as the small molecule lacks the exquisite specificity for CD39 and lacks drug-like properties (46). The major source of extracellular adenosine is the breakdown of ATP, but when that hydrolysis is blocked by an effective anti-CD39, the local ATP generated may have immune-stimulatory effects on the cell expressing both CD39 and ATP receptors, providing a potential explanation for the superiority of anti-CD39 treatment to available antibodies or small-molecule inhibitors of CD73 or A2AR, an argument further bolstered by the requirement for P2X7. However, anti-CD39 could be further enhanced by treatment with an A2ARi. These data suggest that blockade of CD39 ATPase activity was not sufficient to completely abrogate adenosine-mediated immune suppression. One potential explanation is that small quantities of adenosine may be generated by a CD38-driven salvage pathway (41) and suggests a rational clinical strategy for cotargeting CD39 and A2AR.

Although BM-derived CD39 was critical in the antimetastatic activity of anti-CD39, NK cell CD39 was dispensable for the observed antimetastatic activity. Further studies using conditional CD39-floxed strains discriminated that myeloid cell CD39 was necessary for anti-CD39 activity and, in part, explained the reduction in metastasis in the *Cd39<sup>-/-</sup>* mice compared with WT mice. CD39 expressed by NK cells was also not a major regulator of experimental metastases. Instead, multiple lines of evidence pointed to myeloid expressed CD39 as a *cis* mechanism limiting the impact of eATP in driving intratumor myeloid pyroptosis and the release of IL18, both of which could stimulate NK

## New Mechanism of Anti-CD39 Control of Metastases



cell effector function. First, the requirement for host inflammasome components, including ASC and NALP3, was consistent with the P2X7-mediated sensing of ATP in a myeloid-specific manner. Second, either depletion of clodronate-sensitive myeloid cells or neutralization of myeloid cell migration using anti-CD11b was able to abolish the antimetastatic activity of anti-CD39 antibody, further bolstering this argument. We have previously shown that all of these populations have increased CD39 expressed within the metastatic lung TME (10), and in particular a reduction in alveolar macrophages coexpressing CD39 and P2X7 was seen in tumor-burdened lungs immediately post anti-CD39 therapy.

Our data also suggest a potential stimulatory role of local ATP in promoting immunity via pyroptosis. P2X7–NLRP3-mediated pyroptosis in macrophages has been described in other disease contexts (47), and it is possible that myeloid cells can undergo pyroptosis and release IL18 post anti-CD39 treatment. Our experiments *in vitro* with BM macrophages suggest that they are sensitive to anti-CD39-mediated pyroptosis, including caspase-1 activation and IL1 $\beta$  and IL18 release (12). In fact, IL18 and IL18R, but not IL1 $\beta$ , were found to be critical mediators of the anti-CD39-mediated inhibition of metastases. Although IL18 has previously been shown to promote myeloid suppressor cell activity in certain tumor settings (29), its effects appear to be context dependent. In the setting of metastasis prevention, the dominant function of IL18 appears to be its ability to promote NK cell effector functions (18). IL18 has been implicated as a central cytokine in supporting myeloid–NK cell cross-talk by inducing the expression of the IL12 receptor and enhancing IFN $\gamma$  secretion (48, 49). The role of this anti-CD39-driven eATP–P2X7–NALP3–IL18 pathway is consistent with a similar mechanism we have described in CD8<sup>+</sup> T cell-mediated control of subcutaneously implanted tumors (12). At this point, we cannot rule out a *trans* effect of ATP on NK cells via NK cell-expressed P2X7. However, we were able to detect only minimal expression of this purinergic receptor on NK cells in the lungs. We evaluated only host P2X7 deficiency, and many other studies suggest that P2X7 also has protumor activities (50, 51), including prometastatic and proliferative roles when expressed by tumor cells (52, 53) and other impacts on the TME (54). Future experiments will determine the key source of P2X7 contributing to CD39 blockade.

Herein, we also demonstrated the efficacy of combining adjuvant anti-CD39 and anti-PD-1 therapy to improve survival of mice with surgically resected tumors. This approach needs to be extensively

**Figure 7.**

Anti-CD39 controls tumor metastases in combination with other NK cell-activating agents. **A**, Groups ( $n = 10$ –11/group) of B6 WT mice were injected i.v. with LWT1 ( $7.5 \times 10^5$ ) cells on day 0 and treated i.p. with clg (200  $\mu$ g), anti-CD39 (200  $\mu$ g on days 0 and 3), PBS, or IL2 (100,000 IU i.p. on days 0, 1, 2, and 3) or combination of anti-CD39 and IL2 (same dose schedule). **B**, Groups ( $n = 10$ /group) of B6 WT mice were injected i.v. with LWT1 ( $7.5 \times 10^5$ ) cells on day 0 and treated i.p. with clg (200  $\mu$ g), anti-CD39 (200  $\mu$ g on days 0 and 3), PBS, or IL15/IL15R $\alpha$  (0.5  $\mu$ g and 3  $\mu$ g, respectively, on days 0, 1, 2, and 3) or combination of anti-CD39 and IL15/IL15R $\alpha$  (same dose schedule). **C**, Groups ( $n = 10$ /group) of B6 WT mice were injected i.v. with LWT1 ( $7.5 \times 10^5$ ) cells on day 0 and treated i.p. with clg (200  $\mu$ g), anti-CD39 (200  $\mu$ g), vehicle, SCH58261 (A2ARi), or their combination on days 0 and 3 relative to tumor inoculation. The metastatic burden was quantified in the lungs after 14 days by counting colonies on the lung surface. Mean  $\pm$  SEM are shown. Experiments were performed once unless indicated. Significant differences among various treatment groups were determined by one-way ANOVA, followed by the Tukey multiple comparison test (\*,  $P < 0.05$ ; \*\*\*,  $P < 0.001$ ; \*\*\*\*,  $P < 0.0001$ ).

Yan et al.

tested in a neoadjuvant context (24, 55). In experimental models where NK cells are critical, the antimetastatic activity of IL2 and IL15, which promote the expansion and survival of NK cells, was significantly enhanced by anti-CD39, suggesting additional rational clinical combination therapies for anti-CD39 treatment of metastatic disease.

### Disclosure of Potential Conflicts of Interest

S.C. Robson is a consultant for AbbVie, eGenesis, and PureTech, reports receiving commercial research grants from xRx and Tizona Therapeutics, reports receiving other commercial research support from Tizona Therapeutics and eBiosciences/Thermo Fisher, has ownership interest (including patents) in Purinomia and ePURINES, and has provided expert testimony for Morrison Mahoney LLP. C. Beers is Chief Scientific Officer at and has ownership interest (including patents) in Tizona Therapeutics. A.K. Moesta is Director, Immunology at and has ownership interest (including patents) in Tizona Therapeutics. M.W.L. Teng is a consultant for Tizona Therapeutics. M.J. Smyth reports receiving commercial research grants from Bristol-Myers Squibb and Tizona Therapeutics and is a consultant/advisory board member for Tizona Therapeutics. No potential conflicts of interest were disclosed by the other authors.

### Authors' Contributions

**Conception and design:** X.-Y. Li, S.C. Robson, C. Beers, A.K. Moesta, M.W.L. Teng, M.J. Smyth

**Development of methodology:** J. Yan, X.-Y. Li, A. Roman Aguilera, M.J. Smyth  
**Acquisition of data (provided animals, acquired and managed patients, provided facilities, etc.):** J. Yan, X.-Y. Li, A. Roman Aguilera, C. Xiao, C. Jaberger-Foissac, B. Nowlan, S.C. Robson, M.J. Smyth

### References

- Lopez-Soto A, Gonzalez S, Smyth MJ, Galluzzi L. Control of metastasis by NK cells. *Cancer Cell* 2017;32:135–54.
- Vijayan D, Young A, Teng MWL, Smyth MJ. Targeting immunosuppressive adenosine in cancer. *Nat Rev Cancer* 2017;17:709–24.
- Kroemer G, Galluzzi L, Kepp O, Zitvogel L. Immunogenic cell death in cancer therapy. *Annu Rev Immunol* 2013;31:51–72.
- Young A, Mittal D, Stagg J, Smyth MJ. Targeting cancer-derived adenosine: new therapeutic approaches. *Cancer Discov* 2014;4:879–88.
- Di Virgilio F, Falzoni S, Giuliani AL, Adinolfi E. P2 receptors in cancer progression and metastatic spreading. *Curr Opin Pharmacol* 2016;29:17–25.
- Cekic C, Linden J. Purinergic regulation of the immune system. *Nat Rev Immunol* 2016;16:177–92.
- Stagg J, Divisekera U, Duret H, Sparwasser T, Teng MW, Darcy PK, et al. CD73-deficient mice have increased antitumor immunity and are resistant to experimental metastasis. *Cancer Res* 2011;71:2892–900.
- Mittal D, Young A, Stannard K, Yong M, Teng MW, Allard B, et al. Antimetastatic effects of blocking PD-1 and the adenosine A2A receptor. *Cancer Res* 2014;74:3652–8.
- Sun X, Han L, Seth P, Bian S, Li L, Csizmadia E, et al. Disordered purinergic signaling and abnormal cellular metabolism are associated with development of liver cancer in Cd39/ENTPD1 null mice. *Hepatology* 2013;57:205–16.
- Zhang H, Vijayan D, Li XY, Robson SC, Geetha N, Teng MWL, et al. The role of NK cells and CD39 in the immunological control of tumor metastases. *Oncoimmunology* 2019;8:e1593809.
- Beavis PA, Divisekera U, Paget C, Chow MT, John LB, Devaud C, et al. Blockade of A2A receptors potently suppresses the metastasis of CD73+ tumors. *Proc Natl Acad Sci U S A* 2013;110:14711–6.
- Li X, Moesta AK, Xiao C, Nakamura K, Casey M, Zhang H, et al. Targeting CD39 in cancer reveals an extracellular ATP- and inflammasome-driven tumor immunity. *Cancer Discov* 2019;9:1754–73.
- Enjyoji K, Sevigny J, Lin Y, Frenette PS, Christie PD, Esch JS 2nd, et al. Targeted disruption of cd39/ATP diphosphohydrolase results in disordered hemostasis and thromboregulation. *Nat Med* 1999;5:1010–7.
- Young A, Ngiow SF, Barkauskas DS, Sult E, Hay C, Blake SJ, et al. Co-inhibition of CD73 and A2AR adenosine signaling improves anti-tumor immune responses. *Cancer Cell* 2016;30:391–403.

**Analysis and interpretation of data (e.g., statistical analysis, biostatistics, computational analysis):** J. Yan, X.-Y. Li, A. Roman Aguilera, C. Jaberger-Foissac, B. Nowlan, C. Beers, A.K. Moesta, N. Geetha, M.J. Smyth  
**Writing, review, and/or revision of the manuscript:** X.-Y. Li, S.C. Robson, C. Beers, A.K. Moesta, N. Geetha, M.W.L. Teng, M.J. Smyth  
**Administrative, technical, or material support (i.e., reporting or organizing data, constructing databases):** A. Roman Aguilera, N. Geetha  
**Study supervision:** M.W.L. Teng, M.J. Smyth

### Acknowledgments

The authors wish to thank Liam Town, Brodie Quine, and Andreea Zaharia for genotyping and maintenance and care of the mice used in this study. We thank Irmgard Foerster and Ana Anderson for providing mouse strains. M.J. Smyth was supported by a National Health and Medical Research Council (NH&MRC) Senior Principal Research Fellowship (1078671) and Program Grant (1132519) and Melanoma Research Alliance Established Investigator Award (611295). M.W.L. Teng was supported by an NH&MRC Project Grant (1120887) and Prostate Cancer Foundation of Australia (NCG0217). Some of the work was supported by a scientific research agreement with Tizona Therapeutics.

The costs of publication of this article were defrayed in part by the payment of page charges. This article must therefore be hereby marked *advertisement* in accordance with 18 U.S.C. Section 1734 solely to indicate this fact.

Received October 4, 2019; revised December 4, 2019; accepted January 14, 2020; published first January 28, 2020.

- Martinon F, Petrilli V, Mayor A, Tardivel A, Tschopp J. Gout-associated uric acid crystals activate the NALP3 inflammasome. *Nature* 2006;440:237–41.
- Solle M, Labasi J, Perregaix DG, Stam E, Petrusova N, Koller BH, et al. Altered cytokine production in mice lacking P2X(7) receptors. *J Biol Chem* 2001;276:125–32.
- Mariathasan S, Newton K, Monack DM, Vucic D, French DM, Lee WP, et al. Differential activation of the inflammasome by caspase-1 adaptors ASC and Ipaf. *Nature* 2004;430:213–8.
- Takeda K, Tsutsui H, Yoshimoto T, Adachi O, Yoshida N, Kishimoto T, et al. Defective NK cell activity and Th1 response in IL-18-deficient mice. *Immunity* 1998;8:383–90.
- Hoshino K, Tsutsui H, Kawai T, Takeda K, Nakanishi K, Takeda Y, et al. Cutting edge: generation of IL-18 receptor-deficient mice: evidence for IL-1 receptor-related protein as an essential IL-18 binding receptor. *J Immunol* 1999;162:5041–4.
- Thomas HE, Irawaty W, Darwiche R, Brodnicki TC, Santamaria P, Allison J, et al. IL-1 receptor deficiency slows progression to diabetes in the NOD mouse. *Diabetes* 2004;53:113–21.
- Li XY, Das I, Lepletier A, Addala V, Bald T, Stannard K, et al. CD155 loss enhances tumor suppression via combined host and tumor-intrinsic mechanisms. *J Clin Invest* 2018;128:2613–25.
- Clausen BE, Burkhardt C, Reith W, Renkawitz R, Forster I. Conditional gene targeting in macrophages and granulocytes using LysMcre mice. *Transgenic Res* 1999;8:265–77.
- Narni-Mancinelli E, Chaix J, Fenis A, Kerdiles YM, Yessaad N, Reynders A, et al. Fate mapping analysis of lymphoid cells expressing the Nkp46 cell surface receptor. *Proc Natl Acad Sci U S A* 2011;108:18324–9.
- Liu J, Blake SJ, Yong MC, Harjunpaa H, Ngiow SF, Takeda K, et al. Improved efficacy of neoadjuvant compared to adjuvant immunotherapy to eradicate metastatic disease. *Cancer Discov* 2016;6:1382–99.
- Haynes NM, Hawkins ED, Li M, McLaughlin NM, Hammerling GJ, Schwendener R, et al. CD11c+ dendritic cells and B cells contribute to the tumoricidal activity of anti-DR5 antibody therapy in established tumors. *J Immunol* 2010;185:532–41.
- Smyth MJ, Crowe NY, Godfrey DI. NK cells and NKT cells collaborate in host protection from methylcholanthrene-induced fibrosarcoma. *Int Immunol* 2001;13:459–63.

## New Mechanism of Anti-CD39 Control of Metastases

27. Koebel CM, Vermi W, Swann JB, Zerafa N, Rodig SJ, Old LJ, et al. Adaptive immunity maintains occult cancer in an equilibrium state. *Nature* 2007;450:903–7.
28. Ghiringhelli F, Apetoh L, Tesniere A, Aymeric L, Ma Y, Ortiz C, et al. Activation of the NLRP3 inflammasome in dendritic cells induces IL-1beta-dependent adaptive immunity against tumors. *Nat Med* 2009;15:1170–8.
29. Nakamura K, Kassem S, Cleynen A, Chretien ML, Guillerey C, Putz EM, et al. Dysregulated IL-18 is a key driver of immunosuppression and a possible therapeutic target in the multiple myeloma microenvironment. *Cancer Cell* 2018;33:634–48.
30. Blake SJ, Stannard K, Liu J, Allen S, Yong MC, Mittal D, et al. Suppression of metastases using a new lymphocyte checkpoint target for cancer immunotherapy. *Cancer Discov* 2016;6:446–59.
31. Ferrari de Andrade L, Ngjow SF, Stannard K, Rusakiewicz S, Kalimutho M, Khanna KK, et al. Natural killer cells are essential for the ability of BRAF inhibitors to control BRAFV600E-mutant metastatic melanoma. *Cancer Res* 2014;74:7298–308.
32. Young A, Ngjow SF, Madore J, Reinhardt J, Landsberg J, Chitsazan A, et al. Targeting adenosine in BRAF-mutant melanoma reduces tumor growth and metastasis. *Cancer Res* 2017;77:4684–96.
33. Roman Aguilera A, Lutzyk VP, Mittal D, Li XY, Stannard K, Takeda K, et al. CD96 targeted antibodies need not block CD96-CD155 interactions to promote NK cell anti-metastatic activity. *Oncoimmunology* 2018;7:e1424677.
34. Martinet L, Ferrari De Andrade L, Guillerey C, Lee JS, Liu J, Souza-Fonseca-Guimaraes F, et al. DNAM-1 expression marks an alternative program of NK cell maturation. *Cell Rep* 2015;11:85–97.
35. Hayakawa Y, Smyth MJ. CD27 dissects mature NK cells into two subsets with distinct responsiveness and migratory capacity. *J Immunol* 2006;176:1517–24.
36. Adinolfi E, Giuliani AL, De Marchi E, Pegoraro A, Orioli E, Di Virgilio F. The P2X7 receptor: a main player in inflammation. *Biochem Pharmacol* 2018;151:234–44.
37. Adinolfi E, Capece M, Franceschini A, Falzoni S, Giuliani AL, Rotondo A, et al. Accelerated tumor progression in mice lacking the ATP receptor P2X7. *Cancer Res* 2015;75:635–44.
38. Chow MT, Sceneay J, Paget C, Wong CS, Duret H, Tschopp J, et al. NLRP3 suppresses NK cell-mediated responses to carcinogen-induced tumors and metastases. *Cancer Res* 2012;72:5721–32.
39. Gombault A, Baron L, Couillin I. ATP release and purinergic signaling in NLRP3 inflammasome activation. *Front Immunol* 2012;3:414.
40. Swanson KV, Deng M, Ting JP. The NLRP3 inflammasome: molecular activation and regulation to therapeutics. *Nat Rev Immunol* 2019;19:477–89.
41. Chen L, Diaio L, Yang Y, Yi X, Rodriguez BL, Li Y, et al. CD38-mediated immunosuppression as a mechanism of tumor cell escape from PD-1/PD-L1 blockade. *Cancer Discov* 2018;8:1156–75.
42. Gao Y, Souza-Fonseca-Guimaraes F, Bald T, Ng SS, Young A, Ngjow SF, et al. Tumor immunoevasion by the conversion of effector NK cells into type 1 innate lymphoid cells. *Nat Immunol* 2017;18:1004–15.
43. Bastid J, Cottalorda-Regairaz A, Alberici G, Bonnefoy N, Eliaou JF, Bensussan A. ENTPD1/CD39 is a promising therapeutic target in oncology. *Oncogene* 2013;32:1743–51.
44. Zhang B, Cheng B, Li FS, Ding JH, Feng YY, Zhuo GZ, et al. High expression of CD39/ENTPD1 in malignant epithelial cells of human rectal adenocarcinoma. *Tumour Biol* 2015;36:9411–9.
45. Hayes GM, Cairns B, Levashova Z, Chinn L, Perez M, Theunissen JW, et al. CD39 is a promising therapeutic antibody target for the treatment of soft tissue sarcoma. *Am J Transl Res* 2015;7:1181–8.
46. Wall MJ, Wigmore G, Lopatar J, Frenguelli BG, Dale N. The novel NTPDase inhibitor sodium polyoxotungstate (POM-1) inhibits ATP breakdown but also blocks central synaptic transmission, an action independent of NTPDase inhibition. *Neuropharmacology* 2008;55:1251–8.
47. Riestra AM, Valderrama JA, Patras KA, Booth SD, Quek XY, Tsai CM, et al. *Trichomonas vaginalis* induces NLRP3 inflammasome activation and pyroptotic cell death in human macrophages. *J Innate Immun* 2019;11:86–98.
48. Walzer T, Dalod M, Robbins SH, Zitvogel L, Vivier E. Natural-killer cells and dendritic cells: "l'union fait la force". *Blood* 2005;106:2252–8.
49. Mingozzi F, Spreafico R, Gorletta T, Cigni C, Di Gioia M, Caccia M, et al. Prolonged contact with dendritic cells turns lymph node-resident NK cells into anti-tumor effectors. *EMBO Mol Med* 2016;8:1039–51.
50. Di Virgilio F, Sarti AC, Falzoni S, De Marchi E, Adinolfi E. Extracellular ATP and P2 purinergic signalling in the tumour microenvironment. *Nat Rev Cancer* 2018;18:601–18.
51. Adinolfi E, De Marchi E, Orioli E, Pegoraro A, Di Virgilio F. Role of the P2X7 receptor in tumor-associated inflammation. *Curr Opin Pharmacol* 2019;47:59–64.
52. Jelassi B, Chantome A, Alcaraz-Perez F, Baroja-Mazo A, Cayuela ML, Pelegrin P, et al. P2X(7) receptor activation enhances SK3 channels- and cystein cathepsin-dependent cancer cells invasiveness. *Oncogene* 2011;30:2108–22.
53. Adinolfi E, Raffaghelli L, Giuliani AL, Cavazzini L, Capece M, Chiozzi P, et al. Expression of P2X7 receptor increases in vivo tumor growth. *Cancer Res* 2012;72:2957–69.
54. De Marchi E, Orioli E, Pegoraro A, Sangaletti S, Portararo P, Curti A, et al. The P2X7 receptor modulates immune cells infiltration, ectonucleotidases expression and extracellular ATP levels in the tumor microenvironment. *Oncogene* 2019;38:3636–50.
55. Liu J, O'Donnell JS, Yan J, Madore J, Allen S, Smyth MJ, et al. Timing of neoadjuvant immunotherapy in relation to surgery is crucial for outcome. *Oncoimmunology* 2019;8:e1581530.

# Cancer Immunology Research

## Control of Metastases via Myeloid CD39 and NK Cell Effector Function

Juming Yan, Xian-Yang Li, Amelia Roman Aguilera, et al.

*Cancer Immunol Res* 2020;8:356-367. Published OnlineFirst January 28, 2020.

**Updated version** Access the most recent version of this article at:  
doi:[10.1158/2326-6066.CIR-19-0749](https://doi.org/10.1158/2326-6066.CIR-19-0749)

**Supplementary Material** Access the most recent supplemental material at:  
<http://cancerimmunolres.aacrjournals.org/content/suppl/2020/01/28/2326-6066.CIR-19-0749.DC1>

**Cited articles** This article cites 55 articles, 20 of which you can access for free at:  
<http://cancerimmunolres.aacrjournals.org/content/8/3/356.full#ref-list-1>

**Citing articles** This article has been cited by 2 HighWire-hosted articles. Access the articles at:  
<http://cancerimmunolres.aacrjournals.org/content/8/3/356.full#related-urls>

**E-mail alerts** [Sign up to receive free email-alerts](#) related to this article or journal.

**Reprints and Subscriptions** To order reprints of this article or to subscribe to the journal, contact the AACR Publications Department at [pubs@aacr.org](mailto:pubs@aacr.org).

**Permissions** To request permission to re-use all or part of this article, use this link  
<http://cancerimmunolres.aacrjournals.org/content/8/3/356>.  
Click on "Request Permissions" which will take you to the Copyright Clearance Center's (CCC) Rightslink site.